

Article

Anticancer and Antimicrobial Activity of Silver Nanoparticles Synthesized from Pods of *Acacia nilotica*

Nuha Suliman Alduraimhem ¹, Ramesa Shafi Bhat ^{2,*} , Sabah Ahmed Al-Zahrani ², Doaa M. Elnagar ¹, Hussah M. Alobaid ¹  and Maha H. Daghestani ^{1,*} 

¹ Department of Zoology, College of Science, King Saud University, Riyadh 11495, Saudi Arabia

² Biochemistry Department, College of Science, King Saud University, P.O. Box 22452, Riyadh 11495, Saudi Arabia

* Correspondence: rbhat@ksu.edu.sa (R.S.B.); mdaghestani@ksu.edu.sa (M.H.D.)

Abstract: Green synthesized silver nanoparticles (AgNPs) have been used against antibiotic-resistant bacteria and chemo-resistant cancer cells. We synthesized AgNPs from *Acacia nilotica* pods, evaluating their antibacterial activity against eight bacterial strains and anticancer efficiency against two colon cancer cell lines, SW620 and SW480. Expression levels of eight genes (*β-catenin*, *APC*, *TP53*, *Beclin1*, *DKK3*, *Axin*, *Cyclin D1*, and *C-myc*) were checked by a reverse transcription-polymerase chain reaction in cancer cells before and after treatment with *A. nilotica* extract and *A. nilotica*-AgNPs. Prepared nanoparticles were characterized through ultraviolet-visible (UV-vis), Zetasizer, scanning electron microscopy (SEM), and transmission electron microscopy (TEM). Fourier transform infrared spectroscopy (FTIR) was used to identify the functional group in extracts. At first, AgNPs were confirmed by a sharp peak of surface plasmon resonance at 375 nm. The Z-average size was 105.4 nm with a polydispersity index of 0.297. TEM showed particle size of 11–30 nm. The prepared AgNPs showed promising antibacterial activity against bacterial strains and cytotoxic activity against the cancer cell lines. Expression levels of all the genes were affected by extract and AgNPs treatment. Overall, this study recommended both *A. nilotica* pods and *A. nilotica*-AgNPs as attractive candidates for antibacterial and anticancer applications.

Keywords: *Acacia nilotica*; silver nanoparticles; antibacterial activity; cytotoxicity; gene expression



Citation: Alduraimhem, N.S.; Bhat, R.S.; Al-Zahrani, S.A.; Elnagar, D.M.; Alobaid, H.M.; Daghestani, M.H. Anticancer and Antimicrobial Activity of Silver Nanoparticles Synthesized from Pods of *Acacia nilotica*. *Processes* **2023**, *11*, 301. <https://doi.org/10.3390/pr11020301>

Academic Editor: Yi Lu

Received: 15 December 2022

Revised: 11 January 2023

Accepted: 14 January 2023

Published: 17 January 2023



Copyright: © 2023 by the authors. Licensee MDPI, Basel, Switzerland. This article is an open access article distributed under the terms and conditions of the Creative Commons Attribution (CC BY) license (<https://creativecommons.org/licenses/by/4.0/>).

1. Introduction

Nanoscience is one of the outstanding areas of science that utilizes and develops structures and materials with sizes ranging in a nanometer scale. Nano-size ranges between 1 to 100 nm are considered nanoparticles (NP) [1]. Since the emergence of nanotechnology, numerous physical techniques have emerged to synthesize NPs, including laser ablation, electron irradiation, photochemical methods, and chemical reductions; NPs have wide applications, such as in health care, cosmetics, environmental health, mechanics, optics, and biomedical sciences [2,3]. At present, metal-based nanoparticles, such as silver, copper, iron, gold, titanium, platinum, etc., have a primary role in nano-medicine applications [4]. Among them, silver nanoparticles (AgNPs) are the most widely utilized material because of their unique properties [5]. Although the silver ions can be converted to AgNPs by being reduced through a chemical process or by ion sputtering, these techniques need hazardous chemicals for the conversion process, resulting in environmental deterioration [2]. Extracts from many biological sources have the capacity to reduce silver ions to AgNPs with less toxicity and can also act as stabilizing agents during the green-synthesis process [6–10].

AgNPs are reported to be antimicrobial agents against many antibiotic-resistant bacteria as well as having cytotoxic effects against many cancer cells [11]. Green-synthesized AgNPs are being used in different healthcare sectors, especially as antibacterial and anti-cancer agents. The synergistic effect of AgNPs with antibiotics is currently used against

infections caused by multi-resistant gram-positive and gram-negative bacterial strains. Mixing AgNPs with antibiotics reduces the dose required and produces fewer side effects. Antibiotic efficiency is also increased when AgNPs are used as drug carriers, improving their release and selectivity against resistant strains. Many studies have validated the outstanding anticancer potential of green-synthesized AgNPs, as they can target cancer tissue both passively and actively [12]. AgNPs penetrate the cancer tissues, resulting in cell death through activating many signaling pathways related to mitochondrial dysfunction, oxidative stress, autophagy, and endoplasmic reticulum stress [13,14]. Due to their unique size and morphology, green-synthesized AgNPs act as excellent antibacterial agents [15,16]. The mechanism involved in the antibacterial action is not fully understood, but the cations released by AgNPs are able to chelate DNA strands, induce protein damage, and interrupt bacterial cell walls, which leads to elevated reactive oxygen species (ROS) inside the living cells [17–20]. The biological activity, including anticancer and antibacterial properties, of green-synthesized AgNPs is determined by their size and shape [21–24].

Colorectal cancer (CRC) stands in the third position among malignant tumors in humans, with the mortality rate increasing globally and the survival rate remaining low [25]. Treatment resistance in CRC remains an unsolved problem. Metastatic colorectal cancer is mainly treated with chemotherapy of 5-fluorouracil, leucovorin, and oxaliplatin as a first-line drug treatment, but chemoresistance and disease relapse remain a challenge [26]. Nowadays, bacterial antimicrobial resistance has become a leading threat in the health sector. Detergents and disinfectants are supplemented with AgNPs as antimicrobial agents against resistant pathogenic microbes for better hygiene [27].

The *Acacia nilotica* is widely distributed in Egypt, South Africa, India, Australia, and Central America. It is a valuable plant with medicinal properties, and it is potentially rich in antioxidant substances [28]. The entire plant is enriched with biomolecules, such as amino acids, proteins, sugars, and antioxidants. It is also rich in gallic acid, eleagic acid, isoquercetin, leucocyanidolum, and glucopyranoside, and is used for treating many diseases due to its antimicrobial, antiplasmodial, and antioxidant properties. Phenolic compounds present in this plant have the capacity to block or suppress carcinogens and significantly inhibits the development of tumors [29]. As reported by Ali & Qaiser [30], *A. nilotica* can precipitate bacterial proteins to inhibit their growth due to the depletion of nutritional proteins. *A. nilotica* can form irreversible complexes with proline-rich proteins in the bacterial cell to stop protein synthesis [30]. Pods of *A. nilotica* are very rich in protein and essential amino acids. These pods are also enriched with many organic compounds and phytochemicals, such as alkaloids, phenols, resins, steroids, oleosins, phenolics, glycosides, tannins, and volatile essential oils. Although a few studies on the antibacterial and anticancer activity of *A. nilotica* are found in the literature, *A. nilotica* species grown in Saudi Arabia have not been explored. The climatic conditions in deserts induce different biochemical and physiological activities that affect plant growth, development, and production of several metabolites, especially regarding the high content of natural antioxidants (mostly phenolic compounds), hydrocarbons, and terpenoids [31,32]. In the present study, AgNPs were synthesized using an extract of pods of *Acacia nilotica* from Saudi Arabia, and explored for anticancer and antibacterial activity. Expression levels of eight genes (β -catenin, APC, TP53, Beclin1, DKK3, Axin, Cyclin D1, and C-myc) were checked in colon cancer cell lines SW620 and SW480 before and after the treatment with *A. nilotica* extract and *A. nilotica*-AgNPs.

2. Materials and Methods

2.1. *A. nilotica* Pods Extract

Pods from the *A. nilotica* tree grown in Riyadh city were used for the study. Pods were washed, air-dried, and finally powdered. Dried pods were boiled in distilled water with a ratio of 1:10 weight/volume for 30 min. The solution was cooled, filtered, and stored at 4 °C.

2.2. Preparation of Silver Nanoparticles

The *A. nilotica* pod extract was used to reduce the silver nitrate (AgNO_3) solution to AgNPs. 100 mL of extract was added to the AgNO_3 stock solution to keep its final concentration at 1 mM at room temperature. The reduction was observed through the color change from faint yellow to brown.

2.3. Characterization of *A. nilotica*-AgNPs

The synthesized *A. nilotica*-AgNPs were characterized using different techniques.

2.4. UV/Vis Spectroscopic Analysis

Initially, UV/Vis spectroscopic analysis was done for quick detection of synthesized AgNPs. The sample was monitored for the completion of bio-reduction of Ag^+ in an aqueous solution by noting the absorbance at wavelengths from 300 to 600 nm.

2.5. Scanning Electron Microscope (SEM) and Transmission Electron Microscopy (TEM)

The average size of *A. nilotica*-AgNPs was determined by a transmission electron microscope and scanning electron microscopy. Scanning electron microscopy scans the samples through a beam of electrons for three-dimensional imaging. Due to its high resolution, it is often used in nano-medical research. In transmission electron microscopy, the interior of the sample is visualized through the transmission of a beam of electrons through a small specimen. This technique is considered among the most powerful tools for providing information about nanoparticles.

2.6. Average Particles Size and Zeta Potential Analysis

The Z-average size of *A. nilotica*-AgNPs was determined through dynamic light scattering (DLS) and zeta potential by electrophoretic light scattering (ELS). DLS measures particle size by illuminating the particles with a 633 nm wavelength red laser, at a scattering angle of 173° , a measurement temperature of 25°C , and a medium viscosity of 0.887 mPa s. Zeta potential value helps in understanding the inter-particle interaction forces. Particles in the suspension with low density, smaller size, and with a large negative or positive zeta potential repel each other; the system is relatively stable and resists aggregation.

2.7. Fourier-Transformed Infrared Spectroscopy (FTIR)

Fourier-transformed infrared spectroscopy is typically used to explore different bio-reducing functional groups in a sample. Potassium bromide was used to encapsulate *A. nilotica*-extract and *A. nilotica*-AgNPs for Fourier-transformed infrared spectroscopy. Functional groups present in both extracts were detected in a spectrum from 4000 to 400 cm^{-1} .

2.8. Antibacterial Activity

We measured the antibacterial activity of *A. nilotica*-extract and *A. nilotica*-AgNPs against eight bacterial strains by the well-diffusion method. Test bacteria were provided by the Biochemistry Department at the Science College of King Saud University. Test strains include *Staphylococcus aureus*, *Staphylococcus epidermis*, *Bacillus subtilis*, *Streptococcus pneumonia*, *Escherichia coli*, *Salmonella typhi*, *Pseudomonas aeruginosa*, and *Klebsiella pneumonia*. The bacteria suspensions prepared the day before were aseptically spread on nutrient agar plates using a sterile cotton swab. Once dried for a few minutes, a 6 mm well was inserted in the plate with the help of sterile glass rod. For the antibacterial test, each well was loaded with $100\ \mu\text{L}$ of *A. nilotica*-extract or *A. nilotica*-AgNPs. The prepared plates were incubated at 37°C for 18 h. The maximum zone of inhibition was recorded as the diameter in mm for each well.

2.9. Cytotoxic Activity

Cytotoxic activity was measured against two colon cancer cell lines by the MTT assay. SW620, and SW480 colon cancer cell lines were treated with different concentrations (3.125, 6.25, 12.5, 25, 50, and 100 μ L) of *A. nilotica*- extract and *A. nilotica*-AgNPs, and compared with untreated cells to check the cell viability after 24, 48 and 72 h duration. Briefly, 96-well plates were used to seed SW620 and SW480 colon cancer cells at a density of 2×10^5 cells/well for 24 h. Seeded cells were exposed to different test concentrations of *A. nilotica*- extract and *A. nilotica*-AgNPs as mentioned above. Finally, 100 μ L of 3-(4,5-dimethylthiazol-2-yl)-2,5-diphenyltetrazolium bromide (MTT) at a concentration of 5 mg/mL was added at 37 °C. After 2 h of incubation in dark conditions, MTT was removed, followed by the addition of 100 μ L dimethyl Sulphoxide to dissolve formazan crystals. The optical density was recorded at 490 nm.

2.10. Gene Expression

The expression level of eight genes (β -catenin, APC, TP53, Beclin1, DKK3, Axin, Cyclin D1, and C-myc) before and after the treatment with 25 μ m of *A. nilotica*-extract and *A. nilotica*-AgNPs for 48 h was measured using the RT-PCR by using ABI 7500 Sequence Detection System (Applied Biosystems, Foster City, CA, USA). Primer sequences and annealing temperature for RT-PCR are listed in Table 1.

Table 1. Primer sequence used for relative mRNA expression levels.

| Primer | Sequence |
|--------|---|
| GAPDH | F: AATGGGCAGCCGTTAGGAAA R:GCCCAATACGACCAAATCAGAG |
| CCND1 | F: ATCAAGTGTGACCCGGACTG R: CTTGGGGTCCATGTTCTGCT |
| C-MYC | F: TGAAAACAGCCTCCCG R: TTCTCCTCCTCGTCGCAGTA |
| CTNNB1 | F: GTAAAACGACGGCCAGTGGACTTCACCTGACAGATCCA R: CAGGAAACAGCTATGACCAGCTCATCATCCAGCTCCAG |
| APC | F: GACTCGGAAATGGGGTCCAA R: TCTTCAGTGCCTCAACTTGCT |
| BECN1 | F: GTAAAACGACGGCCAGTGTGTTTGGAGATCTTAGAGCAA R: CAGGAAACAGCTATGACCAGCTCATCATCCAGCTCCAG |
| TP53 | F: GTAAAACGACGGCCAGTGTCTGGGCTTCTTGCAATTCT R: CAGGAAACAGCTATGACCCCAAATACTCCACACGCAAA |
| DKK3 | F: GAAGGAGCCACGAGTGCAT R: CAGTGACCCACAGACACACAG |
| AXIN1 | F: GTGCCCTACCTCACATTCC R: CTCACCTTCTCCTCCATGC |

2.11. Statistical Analysis

Results are presented as mean \pm SD for at least three independent experiments. Statistical analyses were performed using SPSS software (version 25.0). Statistical differences between the groups were analyzed through ANOVA and *t*-tests; $p < 0.05$ was considered significant.

3. Results and Discussion

3.1. Green Synthesis of Silver Nanoparticles

Biosynthesis of silver nanoparticles from *A. nilotica*- extract occurred by adding an aqueous solution of silver nitrate. The color change in the mixture from yellow to brown indicates the formation of AgNPs by reducing silver ions. The *A. nilotica* is very rich in

active biomolecules, especially phenols and antioxidants [29,30], which can act as a reducing agents in the synthesis process. In green synthesis, phytochemicals present in extracts acts as reducing agent for the production of metal nanoparticles. Oxygen produced in the process links the reduced metal ions, resulting in stability and preventing agglomeration.

3.2. Characterization of *A. nilotica*-AgNPs

At first, we used UV-vis spectroscopy to confirm the formation of AgNPs with the surface plasmon resonance (SPR) peak at 375 nm (Figure 1). Depending on the size and shape, the surface plasmon resonance peak of AgNPs is in the range 370 to 470 nm [33,34]. Silver ions show sharply localized surface plasmon resonance (LSPR) bands due to strong plasmonic interaction with light [35]. Free electrons present in AgNPs can oscillate frequently to produce an SPR absorption band in light waves [36]. The frequency of SPR is determined by the dielectric constant of the medium, in addition to the size and shape of AgNPs. The Z-average size of prepared AgNPs was 105.4 nm, with a polydispersity index (PDI) of 0.297 (Figure 2). Aggregation and uniformity of synthesized particles in a sample are shown by the PDI value. Monodispersed particles have a PDI value of less than 0.1, whereas large size distribution has values above 0.7. ELS analysis showed a zeta potential of -17.1 mV (Figure 3). The TEM image revealed the formation of AgNPs from *A. nilotica* extract, and was found in the range of 11–26 nm (Figure 4). These results are in agreement with the UV-vis peak of 375 nm, as the plasmon resonance (SPR) peak range depends on the size of the particle, as smaller particles absorb smaller wavelengths [37]. The Z-average size of 105.4 nm indicates little aggregation, as DLS shows hydrodynamic diameter, but images of nanoparticles under TEM are in the dried form [38]. The size difference between the two techniques is acceptable, as in DLS the diameter of the particle is measured with a layer of solvent in the dispersed phase, but not in TEM [21,23]. Surface morphology was determined with SEM. The synthesized AgNPs were distributed irregularly, having rough surfaces (Figure 5). The synthesized AgNPs were stored at room temperature in a dark container to ensure stability and long-term storage [39]. Prior to the antibacterial activity measurement and cytotoxic test mentioned below, we ensured the stability of synthesized nanoparticles by measuring their λ_{\max} values, i.e., the position of the peak.

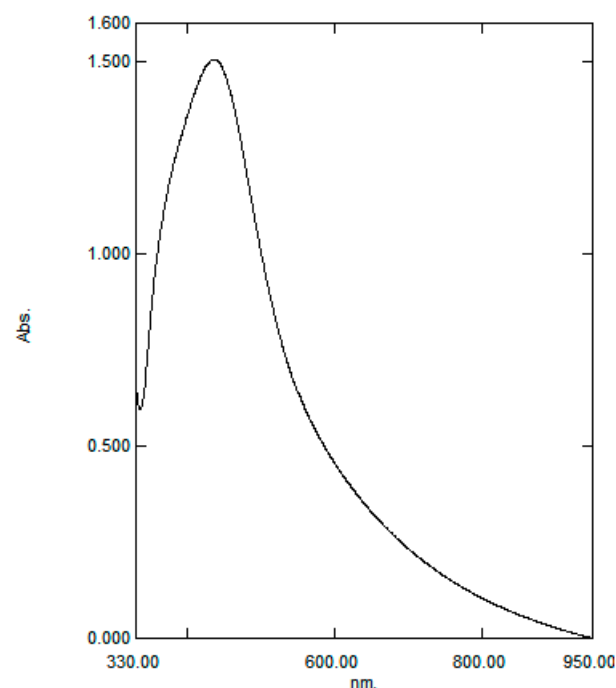


Figure 1. UV-vis absorbance spectra of AgNPs prepared with aqueous *A. nilotica* pod extract.

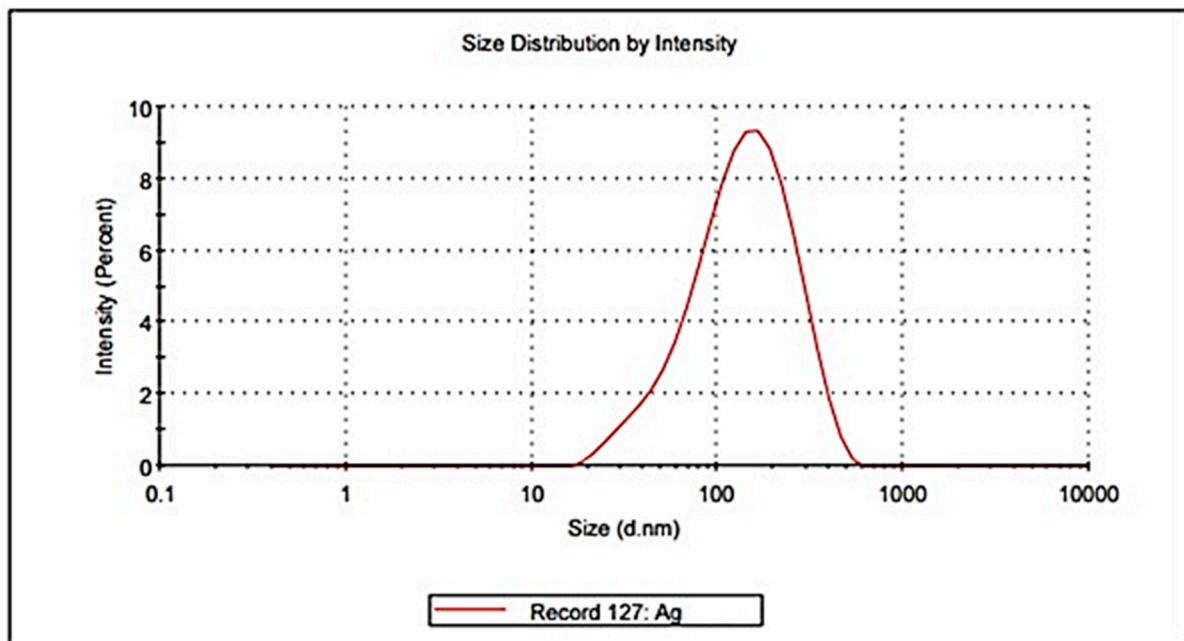


Figure 2. Average size of AgNPs prepared with aqueous *A. nilotica* pod extract.

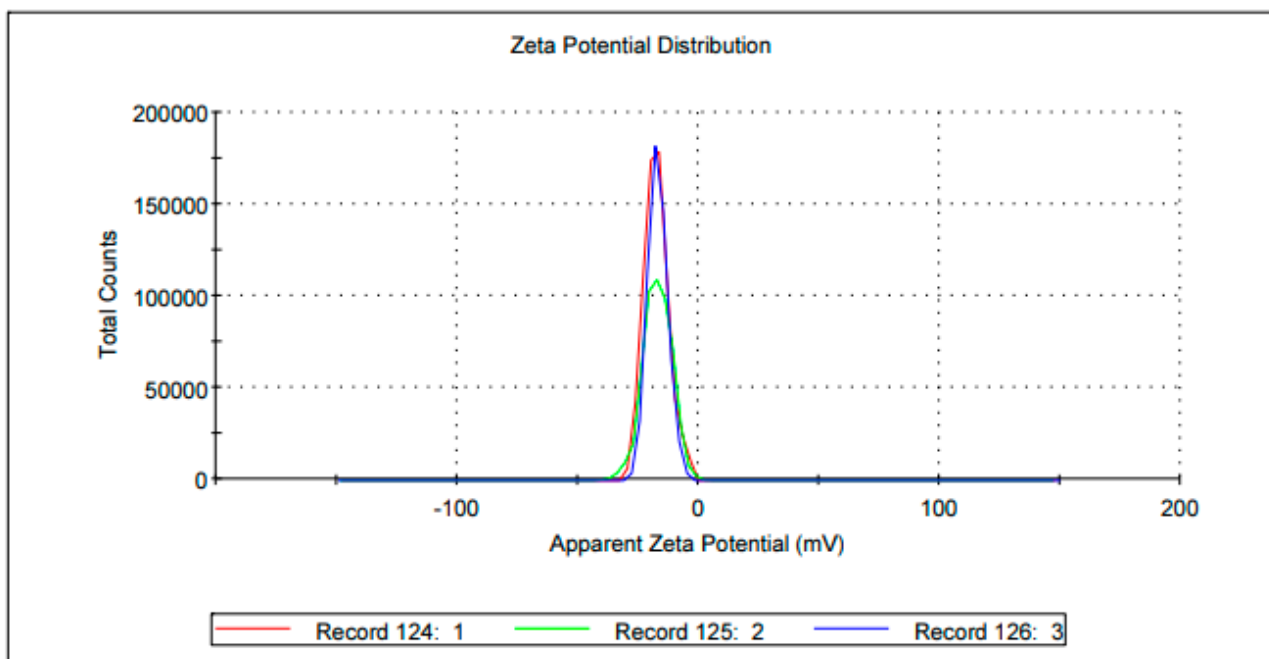


Figure 3. Zeta potential of AgNPs prepared with aqueous *A. nilotica* pod extract.

3.3. Fourier-Transformed Infrared (FTIR)

Many active compounds were detected in *A. nilotica* extract through FTIR, which aided in the green synthesis of nanoparticles (Figure 6). An intense peak is shown for OH stretching due to phenols; N-H and C-H bending for amide and aromatic groups; and C=C stretch for carboxylic or amide groups, representing the presence of active compounds responsible for capping and reducing the particles (Table 2). The spectral data indicate the presence of lipids, proteins, carbohydrates, and pigments [40].

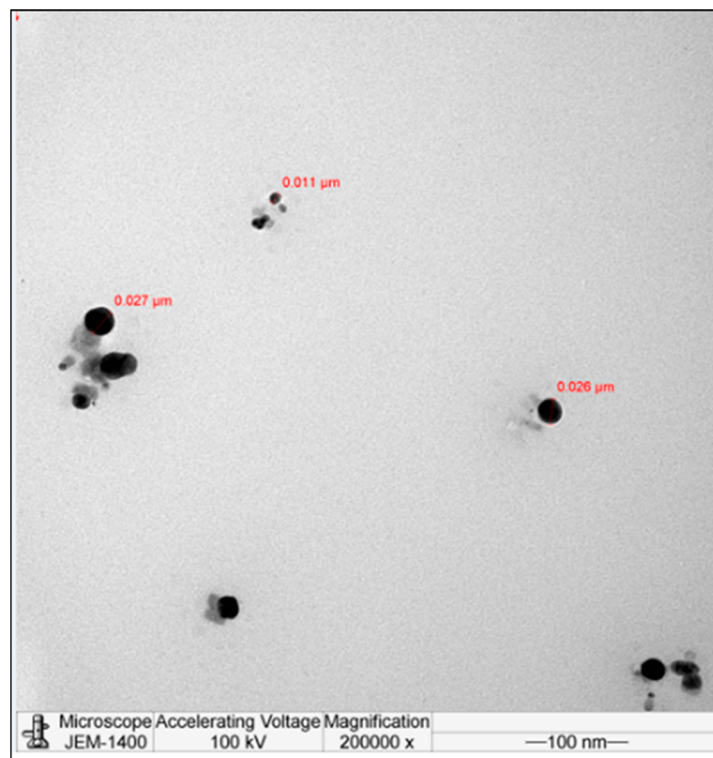


Figure 4. TEM micrograph of AgNPs prepared with aqueous *A. nilotica* pod extract.

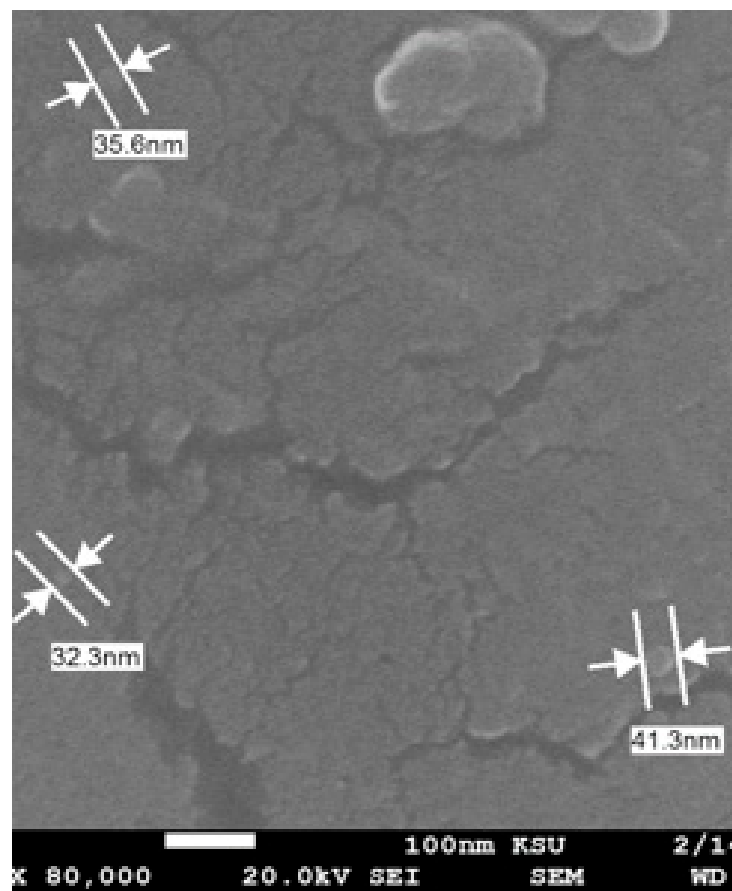


Figure 5. SEM micrograph of AgNPs prepared with aqueous *A. nilotica* pod extract.

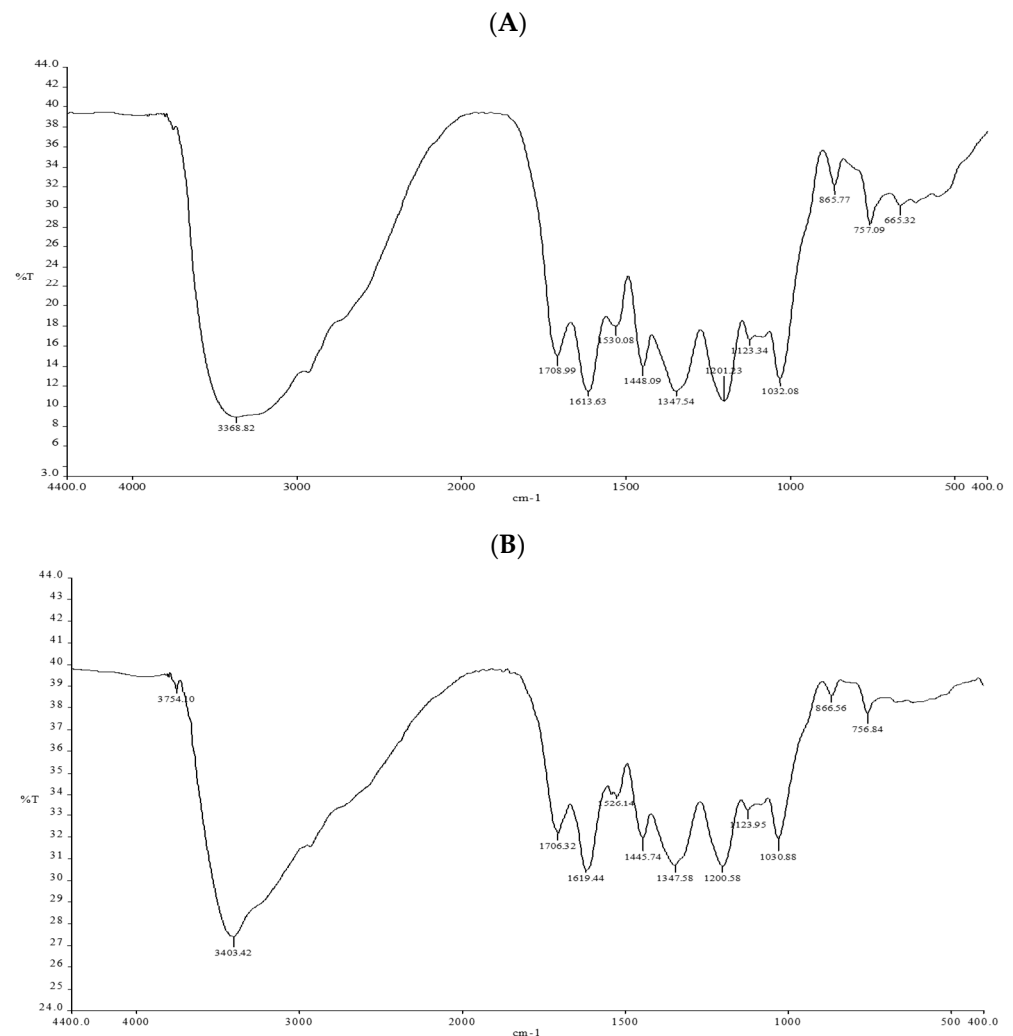


Figure 6. FTIR of (A). Aqueous *A. nilotica* pod extract, (B) Biosynthesized AgNPs prepared with aqueous extract of *A. nilotica* pods.

3.4. Antibacterial Activity

In the present study, eight bacterial strains were tested for the antibacterial efficiency of *A. nilotica* extract and prepared AgNPs. The antibacterial efficiency of both samples shows a varying degree of inhibition for all strains, as shown in Table 3 and Figure 7. Prepared AgNPs were more potent against *E. coli*, with a zone of inhibition of 27 mm, whereas *A. nilotica* extract showed maximum inhibition against *B. subtilis* with 20 mm inhibition zone. Against *S. aureus*, *S. epidermidis*, *S. pneumoniae*, *S. typhi*, *P. aeruginosa*, and *K. pneumoniae*, the zone of inhibition was 20 mm, 23 mm, 25 mm, 25 mm, 15 mm, and 18 mm for AgNPs, respectively, and 10 mm, 11 mm, 13 mm, 12 mm, 10 mm, and 15 mm for *A. nilotica* extract, respectively. The antibacterial efficacy of AgNPs mainly depends on their size and shape, as small-sized and round-shaped particles are more toxic. Many studies have reported round-shaped nanoparticles, with sizes around 10 nm, are efficient antibacterial agents [41]. Plant-derived AgNPs can permeate the bacterial cell, where they can interact with proteins, enzymes, and DNA, leading to cell death. These particles easily stick to the negatively charged bacterial cell surfaces to induce certain chemical and physical changes in the cell boundaries [42]. *A. nilotica*-AgNPs showed a higher inhibition zone against both gram-positive and gram-negative bacterial strains compared with *A. nilotica* extract, which can be related to the small size of the nanoparticles. Several pathogenic gram-positive and gram-negative strains can cause many complications in humans and animals. *Bacillus*, *Staphylococcus*, and *Streptococcus* are members of the most infectious

gram-positive strains, while *Escherichia*, *Klebsiella*, and, *Pseudomonas* are among the most infectious gram-negative strains. Massive application of antibiotics creates drug resistance in many bacterial strains, such as *S. aureus*, *B. subtilis*, *E. coli*, *K. pneumonia*, and *P. aeruginosa*. Use of AgNPs to target resistant bacterial strains as an alternative to antibiotics is of peak interest in the medical field.

Table 2. FT-IR spectra showing probable functional groups of aqueous *A. nilotica* pod extract and *A. nilotica*-AgNPs extract.

| Wave Number (cm ⁻¹) | | Probable Functional Group |
|--|---------------------------|---|
| <i>A. nilotica</i> Extract | <i>A. nilotica</i> -AgNPs | |
| Lipids (3000–2800 cm ⁻¹) | | |
| | 3754.10 | O__H stretch (Alcohols) |
| 3368.82 | 3403.42 | N__H stretch (Amines) |
| Proteins (1700–1500 cm ⁻¹) | | |
| 1708.99 | 1706.32 | C=O (Saturated Aldehyde), C=C stretch (Benzene) |
| 1613.63 | 1619.44 | N__H bend (Nitro compounds, Amides), C__C stretch (Amides), C=O stretch (Carboxylic acid, Ketone), C=C (Benzene, Alkenes) |
| 1530.08 | 1526.04 | N__H bend (Nitro compounds), C__O stretch (Amides, Ketone), C=C (Benzene) |
| Carbohydrates (1500–1200 cm ⁻¹) | | |
| 1448.09 | 1445.75 | N=O stretch (Nitro compounds), CO__H bend (Aldehydes), O__H bend (Alcohols) |
| 1347.54 | 1347.58 | C__N stretch (Amines), C__O stretch (Esters), C__O stretch (Ethers, Alcohols), O__H band (Carboxylic acids) |
| 1201.23 | 1200.58 | C__N stretch (Amines), C__O stretch (Esters), C__O stretch (Ethers, Alcohols), O__H band (Carboxylic acids) |
| 1123.34 | 1123.95 | S=O stretch (Sulfoxides), C__N stretch (Amines), C__O stretch (Esters, Ether, Alcohol) |
| 1032.08 | 1030.88 | N__H bend (Nitro compounds, Amides), C__C stretch (Amides), C ¹ / ₄ O stretch (Carboxylic acid, Ketone), C ¹ / ₄ C (Benzene, Alkenes) |
| -Cell wall components and chlorophyll (1000–600 cm ⁻¹) | | |
| 865.77 | 866.56 | =C__H bend (Alkenes) (Pectin) |
| 757.09 | 756.84 | C__N stretch (Amines), =C__H bend (Benzene), C__C stretch (Chlorides) |
| 665.32 | | C__N stretch (Amines), =C__H bend (Benzene), C__C stretch (Chlorides) |

Table 3. Zone of inhibition (mm) of AgNPs synthesized from plant extract against different gram +ive and gram –ive bacterial strains.

| | Strains | Zone of Inhibition (mm) | |
|-----------|----------------------|-------------------------|---------------|
| | | Plant Extract | Biogenic AgNP |
| Gram +ive | <i>S. aureus</i> | 10 | 20 |
| | <i>B. subtilis</i> | 20 | 20 |
| | <i>S.epidermidis</i> | 11 | 23 |
| | <i>S.pneumonia</i> | 13 | 25 |
| Gram –ive | <i>E. coli</i> | 11 | 27 |
| | <i>S. typhi</i> | 12 | 25 |
| | <i>P. aeruginosa</i> | 10 | 15 |
| | <i>K. pneumoniae</i> | 15 | 18 |

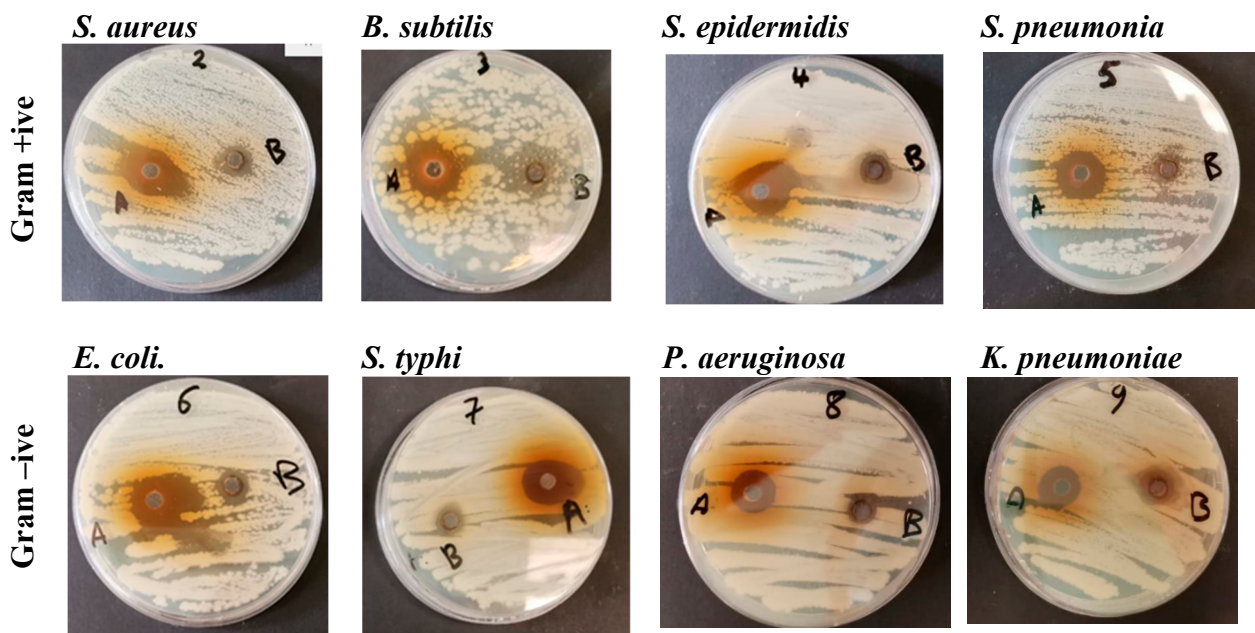


Figure 7. Zone of inhibition (mm) of AgNPs synthesized from plant extract against different gram +ive and gram –ive bacterial strains.

3.5. Cytotoxic Activity

We evaluated in vitro anticancer activity of *A. nilotica* extract (1:10 w/v) and *A. nilotica* AgNPs against two colon cancer cell line, SW620 and SW480. Both samples reduced the cell viability of cancer cells with increased concentration. *A. nilotica* AgNPs showed higher cytotoxicity as compared with *A. nilotica* extract (Figure 8). Both *A. nilotica* extract and AgNPs reduced cell viability at 24 and 48 h. However, cell viability at 72 h was almost the same as at 48 h. This may be due to change in the concentration of extracts over time; after 48 h, the living cells increase their proliferation at lower solvent concentrations, thus causing less toxicity at 72 h of incubation [43,44]. A decrease in cell viability determines the anti-tumor activity of nanoparticles, therefore reducing disease progression [45]. Silver nanoparticles induce cytotoxic effects by physiochemical interaction with intracellular proteins and DNA through phosphate groups and nitrogen bases [46]. AgNPs regulate many signaling pathways in cell cycles by upregulating or downregulating the expression levels of many key genes and reducing cell proliferation and viability [47,48].

3.6. Gene Expression

Mutations in a few genes of the WNT/ β -catenin signaling pathway are detected in CRCs. Therapies inhibiting Wnt/ β -catenin signaling pathways are in clinical trials, but chemo resistance remains a major challenge. Therefore, nanoparticles synthesized from plants are being explored for cancer treatment therapies all over the world. A WNT/ β -catenin signaling pathway is stimulated by activating gene mutations in catenin beta 1 (CTNNB1)-encoding β -catenin, and by inactivating gene mutations in adenomatous polyposis coli (APC) [49]. In the present study, we observed the expression level of key regulators of the Wnt/ β -catenin signaling pathway, besides TP53 and BECN1, after treating the colon-cancer cell lines (SW620 and SW480) with the *A. nilotica* extract and its AgNPs. The expression level of these eight genes, APC, AXIN, DKK3, TP53, CTNNB1, CCND1, C-myc, and BECN1, was measured, as shown in Figure 9.

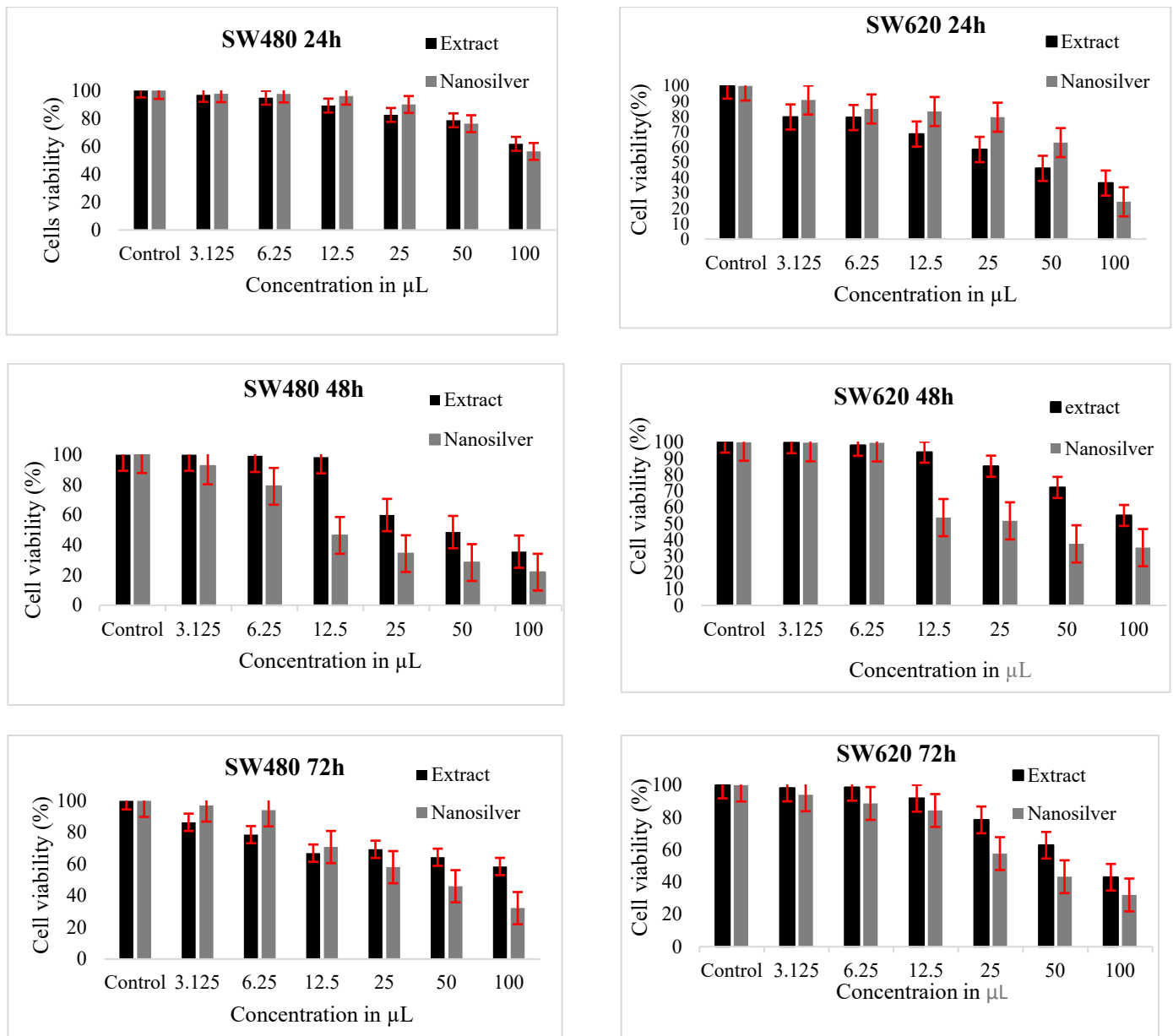


Figure 8. Cytotoxicity of *A.nilotica* pod extract and its AgNPs on colon cancer cell lines (SW480 and SW620) following 24, 48 and 72 h exposure.

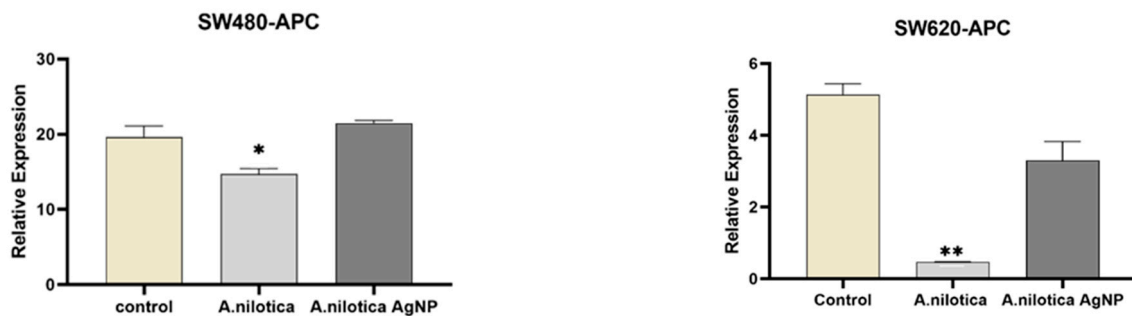


Figure 9. Cont.

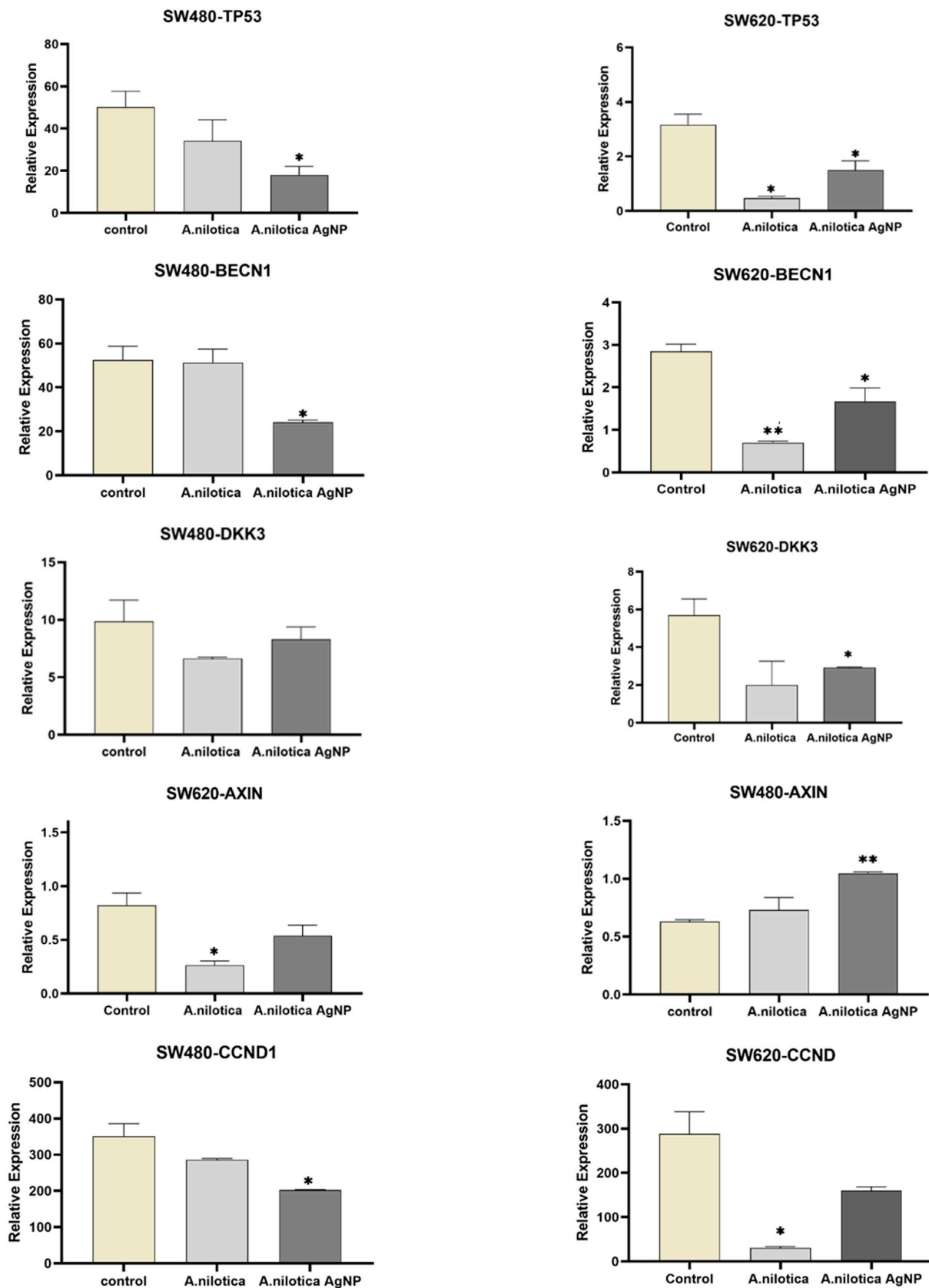


Figure 9. Cont.

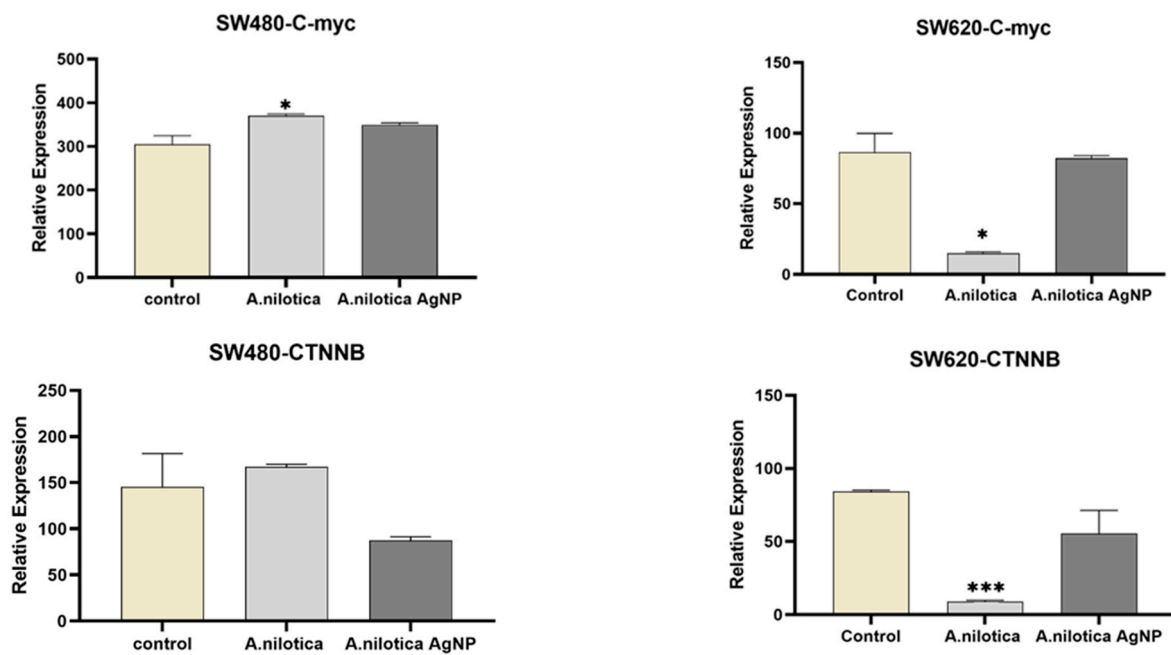


Figure 9. Gene-expression levels in colon cancer cell lines (SW480 and SW620) treated with *A. nilotica* pod extract and AgNPs; control (without treatment) versus treated cell line. * $p \leq 0.05$; ** $p \leq 0.01$; *** $p \leq 0.001$.

Gene-expression results showed a decrease in the expression levels of APC with *A. nilotica* extract treatment, with a slight increase with AgNPs in SW480. However, both treatments decreased the expression in SW620. AXIN showed a significant increase in expression with extract and AgNPs in SW480, but the expression level of both genes was lower in SW620. TP53 and DKK3 expression level was lowered by extract and AgNPs treatment in both colorectal cell lines. CTNNB1, C-myc, CCND1, and BECN1 showed a decrease in expression with *A. nilotica* extract in SW620, but AgNPs treatment decreased the expression level in both cell lines. The reduced expression of AXIN and abnormal expression of CTNNB1, C-myc, CCND1 are used as a marker for determining metastasis [50,51]. Cell lines have their unique characteristics; SW480 cells are derived from the primary tumor, while SW620 cells are derived from a metastatic site [52]. The minor difference in expression levels of genes in both cell lines can be correlated with their origin [53]. Different levels of gene expression in cancer tissue is correlated with tumor size, clinical stage, and pathological grade [54]. Many anticancer agents/therapies target Wnt signaling, as it is mostly dysregulated in cancer tissue. Many such anticancer agents are explored keenly for early-phase clinical trials set up. Some agents with minimally acceptable toxicity have demonstrated abrogation of the pathway. Axin is associated with the colorectal tumor suppressor APC; Axin interacts with b-catenin, GSK-3b, and APC, and negatively regulates the Wnt signaling pathway, presumably by regulating the level of b-catenin [55]. The expression level of Dkk3 is downregulated in colorectal non-neoplastic mucosa, adenoma to adenocarcinoma, and is negatively correlated with invasion depth and colorectal cancer cell dedifferentiation rate [56]. Cyclin D1 is an oncogene that regulates the cell cycle. Cyclin D1 is assumed to play a very important role in cancer development, as it regulates the G1 progression step of the cell cycle. More than one-third of colorectal cancer showed upregulated Cyclin D1 expression [57]. In addition, the disparity in gene-expression results may relate to cell sensitivity and metastatic tumors.

4. Conclusions

This is probably the first report of AgNPs synthesized from pods of *A. nilotica* from Saudi Arabia. *A. nilotica* pods were used as reducing and capping agents for the synthesis

of AgNPs. SPR peak revealed small sized particles, which was confirmed by TEM, in the range of 11–26 nm. FTIR detected intense peak for active compounds responsible for capping and reducing the particles. *A. nilotica*-AgNPs showed remarkable antibacterial and anticancer activity. However, *in vivo* studies through animal models are needed to further elaborate their efficacy.

Author Contributions: N.S.A.: Methodology, literature review, data collection and interpretation, R.S.B.: Writing—original draft; S.A.A.-Z.: Data analysis; D.M.E.: Methodology; H.M.A.: Methodology; M.H.D.: Project administration, design, and supervision. All authors have read and agreed to the published version of the manuscript.

Funding: This research was funded and supported by Researchers Supporting Project number (RSP2023R495) King Saud University, Riyadh, Saudi Arabia.

Data Availability Statement: All the data is present in the manuscript.

Acknowledgments: This research project was supported by Researchers Supporting Project number (RSP2023R495) King Saud University, Riyadh, Saudi Arabia.

Conflicts of Interest: The authors declare that they have no competing interest.

References

1. Khan, I.; Khan, K.S.I. Nanoparticles; Properties, applications, and toxicities. *Arab. J. Chem.* **2019**, *12*, 908–931. [[CrossRef](#)]
2. Yusuf, M. Silver Nanoparticles: Synthesis and Applications. *Handbook of Ecomaterials.* **2018**, 2343–2356. [[CrossRef](#)]
3. Khosravimelal, S.; Chizari, M.; Farhadihosseinabadi, B.; Moghaddam, M.M.; Gholipourmalekabadi, M. Fabrication and characterization of an antibacterial chitosan/silk fibroin electrospun nanofiber loaded with a cationic peptide for wound-dressing application. *J. Mater. Sci. Mater. Med.* **2021**, *32*, 114. [[CrossRef](#)]
4. Yaqoob, A.A.; Ahmad, H.; Parveen, T.; Ahmad, A.; Oves, M.; Ismail, I.M.I.; Qari, H.A.; Umar, K.; MohamadIbrahim, M.N. Recent Advances in Metal Decorated Nanomaterials and Their Various Biological Applications: A Review. *Front. Chem.* **2020**, *8*, 341. [[CrossRef](#)]
5. Hasan, S. A review on nanoparticles: Their synthesis and types. *Res. J. Recent Sci.* **2015**, *4*, 1–3.
6. Bhat, R.S.; Almusallam, J.; Al Daihan, S.; Al-Dbass, A. Biosynthesis of silver nanoparticles using *Azadirachta indica* leaves: characterisation and impact on *Staphylococcus aureus* growth and glutathione-S-transferase activity. *IET Nanobiotechnol.* **2019**, *13*, 498–502. [[CrossRef](#)]
7. Al-Zahrani, S.A.; Bhat, R.S.; Al Rashed, S.A.; Mahmood, A.; Al Fahad, A.; Alamro, G.; Almusallam, J.; Al Subki, R.; Orfali, R.; Al Daihan, S. Green-synthesized silver nanoparticles with aqueous extract of green algae *Chaetomorpha ligustica* and its anticancer potential. *Green Process. Synth.* **2021**, *10*, 711–721. [[CrossRef](#)]
8. Daghestani, M.; Al Rashed, S.A.; Bukhari, W.; Al-Ojayan, B.; Ibrahim, E.M.; Al-Qahtani, A.M.; Merghani, N.M.; Ramadan, R.; Bhat, R.S. Bactericidal and cytotoxic properties of green synthesized nanosilver using *Rosmarinus officinalis* leaves. *Green Process Synth.* **2020**, *9*, 230–236. [[CrossRef](#)]
9. El-Ansary, A.; Warsy, A.; Daghestani, M.; Merghani, N.M.; Al-Dbass, A.; Bukhari, W. Characterization, antibacterial, and neurotoxic effect of green synthesized nanosilver using *Ziziphus spina Christi* aqueous leaf extract collected from Riyadh, Saudi Arabia. *Mater. Res. Exp.* **2018**, *5*, 025033. [[CrossRef](#)]
10. Sayadi, K.; Akbarzadeh, F.; Pourmardan, V.; Saravani-Aval, M.; Sayadi, J.; Chauhan, N.P.S.; Sargazi, G. Methods of green synthesis of Au NCs with emphasis on their morphology: A mini-review. *Heliyon* **2021**, *7*, e07250. [[CrossRef](#)] [[PubMed](#)]
11. Qing, Y.; Cheng, L.; Li, R.; Liu, G.; Zhang, Y.; Tang, X.; Wang, J.; Liu, H.; Qin, Y. Potential antibacterial mechanism of silver nanoparticles and the optimization of orthopedic implants by advanced modification technologies. *Int. J. Nanomed.* **2018**, *13*, 3311–3327. [[CrossRef](#)] [[PubMed](#)]
12. Kovács, D.; Igaz, N.; Gopisetty, M.K.; Kiricsi, M. Cancer Therapy by Silver Nanoparticles: Fiction or Reality? *Int. J. Mol. Sci.* **2022**, *23*, 839. [[CrossRef](#)] [[PubMed](#)]
13. Chen, Y.; Yang, T.; Chen, S.; Qi, S.; Zhang, Z.; Xu, Y. Silver nanoparticles regulate autophagy through lysosome injury and cell hypoxia in prostate cancer cells. *J. Biochem. Mol. Toxicol.* **2020**, *34*, e22474. [[CrossRef](#)]
14. Simard, J.-C.; Durocher, I.; Girard, D. Silver nanoparticles induce irremediable endoplasmic reticulum stress leading to unfolded protein response-dependent apoptosis in breast cancer cells. *Apoptosis* **2016**, *21*, 1279–1290. [[CrossRef](#)]
15. Gherasim, O.; Puiu, R.A.; Birca, A.C.; Burdusel, A.C.; Grumezescu, A.M. An updated review on silver nanoparticles in biomedicine. *Nanomaterials* **2020**, *10*, 2318. [[CrossRef](#)]
16. Kong, I.C.; Ko, K.S.; Koh, D.C. Evaluation of the Effects of Particle Sizes of Silver Nanoparticles on Various Biological Systems. *Int. J. Mol. Sci.* **2020**, *21*, 8465. [[CrossRef](#)]
17. Wang, L.; Hu, C.; Shao, L. The antimicrobial activity of nanoparticles: Present situation and prospects for the future. *Int. J. Nanomed.* **2017**, *12*, 1227–1249. [[CrossRef](#)]

18. Kruszewski, M.; Brzoska, K.; Brunborg, G.; Asare, N.; Dobrzynska, M.; Dusinska, M.; Fjellsbø, L.; Georgantzopoulou, A.; Gromadzka-Ostrowska, J.; Gutleb, A.; et al. Toxicity of silver nanomaterials in higher eukaryotes. *Adv. Mol. Toxicol.* **2011**, *5*, 179–218.
19. Fu, P.P.; Xia, Q.; Hwang, H.M.; Ray, P.C.; Yu, H. Mechanisms of nanotoxicity: Generation of reactive oxygen species. *J. Food Drug Anal.* **2014**, *22*, 64–75. [[CrossRef](#)]
20. Rinna, A.; Magdolenova, Z.; Hudecova, A.; Kruszewski, M.; Refsnes, M.; Dusinska, M. Effect of silver nanoparticles on mitogen-activated protein kinases activation: Role of reactive oxygen species and implication in DNA damage. *Mutagenesis* **2015**, *30*, 59–66. [[CrossRef](#)] [[PubMed](#)]
21. Rizwana, H.; Alwhibi, M.S.; Aldarson, H.A.; Awad, M.A.; Soliman, D.A.; Bhat, R.S. Green synthesis, characterization, and antimicrobial activity of silver nanoparticle prepared using *Trigonella foenum-graecum* L. leaves grown in Saudi Arabia. *Green Process. Synth.* **2021**, *10*, 421–429. [[CrossRef](#)]
22. Almukaynizi, F.B.; Daghestani, M.H.; Awad, M.A.; Althomali, A.; Merghani, N.M.; Bukhari, W.I.; Algahtani, N.M.; Al-Zuhairy, S.S.; AlOthman, A.M.; Alsenani, E.A.; et al. Cytotoxicity of green-synthesized silver nanoparticles by *Adansonia digitata* fruit extract against HTC116 and SW480 human colon cancer cell lines. *Green Process. Synth.* **2022**, *11*, 411–422. [[CrossRef](#)]
23. Al-Zahrani, S.A.; Bhat, R.S.; Al-Onazi, M.A.; Alwhibi, M.S.; Soliman, D.A.; Aljebri, N.A.; Al-Suhaibani, L.S.; Al Daihan, S. Anticancer potential of biogenic silver nanoparticles using the stem extract of *Commiphora gileadensis* against human colon cancer cells. *Green Process. Synth.* **2022**, *11*, 435–444. [[CrossRef](#)]
24. Althomali, A.; Daghestani, M.H.; Almukaynizi, B.; Al-Zahrani, F.; Ahmed, S.; Awad, M.A.; Merghani, N.M.; Bukhari, W.I.; Ibrahim, E.M.; Alzahrani, S.M.; et al. Anti-colon cancer activities of green-synthesized *Moringa oleifera*-AgNPs against human colon cancer cells. *Green Process. Synth.* **2022**, *11*, 545–554. [[CrossRef](#)]
25. Xi, Y.; Xu, P. Global colorectal cancer burden in 2020 and projections to 2040. *Transl. Oncol.* **2021**, *14*, 101174. [[CrossRef](#)] [[PubMed](#)]
26. Zocche, D.M.; Ramirez, C.; Fontao, F.M.; Costa, L.D.; Redal, M.A. Global impact of KRAS mutation patterns in FOLFOX treated metastatic colorectal cancer. *Front. Genet.* **2015**, *6*, 116. [[CrossRef](#)]
27. Deshmukh, S.P.; Patil, S.M.; Mullani, S.B.; Delekar, S.D. Silver nanoparticles as an effective disinfectant: A review. *Mater. Sci. Eng. C Mater. Biol. Appl.* **2019**, *97*, 954–965. [[CrossRef](#)]
28. Osama, A.; AWdelkarim, S.; Fadul, E.; Mohamed, G.; Siddig, M.; Sheikh, A.; Abdelmoneim, A.; Khalid, A.; Hashesh, A.M. In vitro Evaluation of *Acacia nilotica* Pods for its Antioxidant, Acetylcholinesterase Inhibitory. *Eur. Acad. Res.* **2015**, *3*, 2286.
29. Sadiq, M.B.; Tharaphan, P.; Chotivanich, K.; Tarning, J.; Anal, A.K. In vitro antioxidant and antimalarial activities of leaves, pods, and bark extracts of *Acacia nilotica* (L.) Del. *BMC Complement Altern Med.* **2017**, *17*, 372. [[CrossRef](#)]
30. Ali, S.; Qaiser, M. Hybridization in *Acacia nilotica* (Mimosoideae) complex. *Bot. J. Linn. Soc.* **2008**, *80*, 69–77. [[CrossRef](#)]
31. Yeshi, K.; Crayn, D.; Ritmejeriyte, E.; Wangchuk, P. Plant Secondary Metabolites Produced in Response to Abiotic Stresses Has Potential Application in Pharmaceutical Product Development. *Molecules* **2022**, *27*, 313. [[CrossRef](#)]
32. Jamloki, A.; Bhattacharyya, M.; Nautiyal, M.C.; Patni, B. Elucidating the relevance of high temperature and elevated CO₂ in plant secondary metabolites (PSMs) production. *Heliyon* **2021**, *7*, e07709. [[CrossRef](#)] [[PubMed](#)]
33. Zaarour, M.; El Roz, M.; Dong, B.; Retoux, R.; Aad, R. Photochemical preparation of silver nanoparticles supported on zeolite crystals. *Langmuir Am. Chem. Soc.* **2014**, *30*, 6250–6256.
34. Maarebia, R.Z.; Wahab, A.W.; Taba, P. Synthesis and Characterization Of Silver Nanoparticles Using Water Extract of Sarang Semut (*Myrmecodia pendans*) For Blood Glucose Sensors. *J. Akta Kim. Indones. (Indones. Chim. Acta)* **2019**, *12*, 29–46. [[CrossRef](#)]
35. Yguerabide, J.; Yguerabide, E.E. Light-scattering submicroscopic particles as highly fluorescent analogs and their use as tracer labels in clinical and biological applications. *Anal. Biochem.* **1998**, *262*, 137–156. [[CrossRef](#)]
36. Bilal, M.; Rasheed, T.; Iqbal, H.M.; Li, C.; Hu, H.; Zhang, X. Development of silver nanoparticles loaded chitosan-alginate constructs with biomedical potentialities. *Int. J. Biol. Macromol.* **2017**, *105*, 393–400. [[CrossRef](#)]
37. Rahman, A.; Kumar, S.; Bafana, A.; Lin, J.; Dahoumane, S.A.; Jeffryes, C. A Mechanistic View of the Light-Induced Synthesis of Silver Nanoparticles Using Extracellular Polymeric Substances of *Chlamydomonas reinhardtii*. *Molecules* **2019**, *24*, 3506. [[CrossRef](#)]
38. Clayton, K.N.; Salameh, J.W.; Wereley, S.T.; Kinzer-Ursem, T.L. Physical characterization of nanoparticle size and surface modification using particle scattering diffusometry. *Biomicrofluidics* **2016**, *10*, 054107. [[CrossRef](#)]
39. Velgosova, O.; Čížárová, E.; Málek, J.; Kavuličová, J. Effect of storage conditions on long-term stability of Ag nanoparticles formed via green synthesis. *Int. J. Miner. Metall. Mater.* **2017**, *24*, 1177–1182. [[CrossRef](#)]
40. Bhat, R.S.; Alghamdi, J.M.; Aldbass, A.M.; Aljebri, N.A.; Alangery, A.B.; Soliman, D.A.; Al-Daihan, S. Biochemical and FT-IR profiling of *Tritium aestivum* L. seedling in response to sodium fluoride treatment. *Fluoride* **2022**, *55*, 81–89.
41. Rai, M.K.; Deshmukh, S.D.; Ingle, A.P.; Gade, A.K. Silver nanoparticles: The powerful nano weapon against multidrug-resistant bacteria. *J. Appl. Microbiol.* **2012**, *112*, 841–852. [[CrossRef](#)]
42. Nel, A.E.; Mädler, L.; Velegol, D.; Xia, T.; Hoek, E.M.V.; Somasundaran, P.; Klaessig, F.; Castranova, V. Understanding biophysicochemical interactions at the nano-bio interface. *Nat. Mater.* **2009**, *8*, 543–557. [[CrossRef](#)] [[PubMed](#)]
43. Hurley, M.M.; Martin, D.; Raisz, L.G. Changes in ethanol concentration during incubation in multiwell tissue culture trays. *Proc. Soc. Exp. Biol. Med.* **1987**, *186*, 139–141. [[CrossRef](#)]
44. Koc, A.; Karabay, A.Z.; Ozkan, T.; Buyukbingol, Z.; Aktan, F. Time and concentration dependent effects of different solvents on proliferation of K562, HL60, HCT-116 and H929 cell lines. *J. Res. Pharm.* **2022**, *26*, 494–501. [[CrossRef](#)]

45. Malik, P.; Shankar, R.; Malik, V.; Sharma, N.; Mukherjee, T. Green chemistry based benign routes for nanoparticle synthesis. *J. Nanopart.* **2014**, *2014*, 302429. [[CrossRef](#)]
46. Hedberg, J.; Skoglund, S.; Karlsson, M.E.; Wold, S.; Odnevall Wallinder, I.; Hedberg, Y. Sequential studies of silver released from silver nanoparticles in aqueous media simulating sweat, laundry detergent solutions, and surface water. *Environ. Sci. Technol.* **2014**, *48*, 7314–7322. [[CrossRef](#)] [[PubMed](#)]
47. Farah, M.A.; Ali, M.A.; Chen, S.-M.; Li, Y.; Al-Hemaid, F.M.; Abou-Tarboush, F.M.; Al-Anazi, K.M.; Lee, J. Silver nanoparticles synthesized from *Adenium obesum* leaf extract induced DNA damage, apoptosis, and autophagy via generation of reactive oxygen species. *Colloids Surf. B Biointerfaces* **2016**, *141*, 158–169. [[CrossRef](#)]
48. Yang, T.; Yao, Q.; Cao, F.; Liu, Q.; Liu, B.; Wang, X.H. Silver nanoparticles inhibit the function of hypoxia-inducible factor-1 and target genes: Insight into the cytotoxicity and antiangiogenesis. *Int. J. Nanomed.* **2016**, *11*, 6679–6692. [[CrossRef](#)]
49. Schatoff, E.M.; Leach, B.I.; Dow, L.E. Wnt signaling and colorectal cancer. *Curr. Color. Cancer Rep.* **2017**, *13*, 101–110. [[CrossRef](#)]
50. Marcolino, T.F.; Pimenta, C.A.M.; Artigiani Neto, R.; Castelo, P.; Silva, M.S.; Forones, N.M.; Oshima, C.T.F. p53, Cyclin-D1, β -catenin, APC and c-myc in Tumor Tissue from Colorectal and Gastric Cancer Patients with Suspected Lynch Syndrome by the Bethesda Criteria. *Asian Pac. J. Cancer Prev.* **2020**, *21*, 343–348. [[CrossRef](#)]
51. Seiler, R.; Thalmann, G.; Rotzer, D. CCND1/CyclinD1 status in metastasizing bladder cancer: A prognosticator and predictor of chemotherapeutic response. *Mod. Pathol.* **2014**, *27*, 87–95. [[CrossRef](#)] [[PubMed](#)]
52. Thuringer, D.; Berthenet, K.; Cronier, L.; Solary, E.; Garrido, C. Primary tumor- and metastasis-derived colon cancer cells differently modulate connexin expression and function in human capillary endothelial cells. *Oncotarget* **2015**, *6*, 28800–28815. [[CrossRef](#)] [[PubMed](#)]
53. Alamro, G.; Almousa, N.; Almusallam, J.; Watyan, M.B.; Alghamdi, S.; Al-Jabr, S.; Alqahtani, N.; Aldbass, A.; Bhat, R.S.; Daihan, S.A. Gene Expression Analysis of Specific Genes Related to Genomic Stability in Colon Cancer Cell Lines—A Resource for Cancer Research. *J. Pharm. Res. Int.* **2022**, *34*, 10–19. [[CrossRef](#)]
54. Salvadores, M.; Fuster-Tormo, F.; Supek, F. Matching cell lines with cancer type and subtype of origin via mutational, epigenomic, and transcriptomic patterns. *Sci. Adv.* **2020**, *6*, eaba1862. [[CrossRef](#)] [[PubMed](#)]
55. Nakamura, T.; Hamada, F.; Ishidate, T.; Anai, K.-I.; Kawahara, K.; Toyoshima, K.; Akiyama, T. Axin, an inhibitor of the Wnt signaling pathway, interacts with beta-catenin, GSK-3beta and APC and reduces the beta-catenin level. *Genes Cells* **1998**, *3*, 395–403. [[CrossRef](#)]
56. Zhao, S.; Hao, C.-L.; Zhao, E.-H.; Jiang, H.-M.; Zheng, H.-C. The Suppressing Effects of Dkk3 Expression on Aggressiveness and Tumorigenesis of Colorectal Cancer. *Front. Oncol.* **2020**, *10*, 600322. [[CrossRef](#)]
57. Alao, J.P. The regulation of cyclin D1 degradation: Roles in cancer development and the potential for therapeutic invention. *Mol. Cancer* **2007**, *6*, 24. [[CrossRef](#)]

Disclaimer/Publisher’s Note: The statements, opinions and data contained in all publications are solely those of the individual author(s) and contributor(s) and not of MDPI and/or the editor(s). MDPI and/or the editor(s) disclaim responsibility for any injury to people or property resulting from any ideas, methods, instructions or products referred to in the content.